Energy xxx (2015) 1–8

Contents lists available at ScienceDirect

Energy

journal homepage: www.elsevier.com/locate/energy

Modelling of electrical energy consumption in an electric arc furnace using artificial neural networks

Dragoljub Gajic [a, b, *], Ivana Savic-Gajic [c, d], Ivan Savic [c, d], Olga Georgieva [b], Stefano Di Gennaro [d]

[a] School of Electrical Engineering, University of Belgrade, Bulevar kralja Aleksandra 73, 11000 Belgrade, Serbia
[b] Faculty of Mathematics and Informatics, University of Sofia "St. Kl. Ohridski", Tsarigradsko shosse 125, 1113 Sofia, Bulgaria
[c] Faculty of Technology, University of Nis, Bulevar oslobodjenja 124, 16000 Leskovac, Serbia
[d] Center of Excellence DEWS, University of L'Aquila, Via Giovanni di Vincenzo 16, 67100 L'Aquila, Italy

ARTICLE INFO

Article history:
Received 28 February 2015
Received in revised form
14 July 2015
Accepted 15 July 2015
Available online xxx

Keywords:
Multilayer perceptron
Modeling
Electrical energy consumption
Scrap optimization
Electric arc furnace

ABSTRACT

The objective of this research was to use state-of-the-art artificial neural network approach to estimate the extent and effect of fluctuations in the chemical composition of stainless steel at tapping of an electric arc furnace, and thus scrap and alloy weights in the charge material mix, on the specific electrical energy consumption. Such an estimation would help to further evaluate process control strategies and optimize overall operation of the electric arc furnace. The multilayer perceptron architecture 5-5-1 with hyperbolic tangent function in the hidden layer and linear function in the output layer was used as an optimal neural network model. The model was built, tested and validated based on experimental melts of the electric arc furnace at a melt shop in Italy. The proposed model was presented as an adequate one based on the coefficient of determination (R^2) which was above 0.9 as well as other error parameters calculated. The highest effect on the electrical energy consumption has carbon content.

1. Introduction

Stainless steel plays a very important role in the economic development and its consumption per capita has been considered as an index of relative prosperity of a community. Stainless steel is also recognized as a reference for sustainable development because it is 100% recyclable at the end of its life. On the other hand the stainless steel industry is among the most energy-intensive industries where energy has a major share of operating costs and energy savings initiatives play very important role from both economic and environmental point of view [1]. Over the past few years the stainless steel market has become highly competitive. As a result, the highest priority of the latest research work on stainless steel production has been to develop the most advanced models and techniques to produce a given quantity of stainless steel at the lowest possible cost in a stainless steel plant.

The main raw material for production of stainless steel is recycled steel scrap, mostly stainless steel scrap [2]. Around 70–80% recycled scrap is used in the production [3]. The rest is virgin material in the form of different ferro-alloys. To handle such big volumes of scrap, rigorous purchase routines are needed. At arrival, before entering the melt shop site, scrap is tested to ensure that no radioactive components are present. Scrap is then tested, analyzed and sorted according to its alloying element content to ensure that as little virgin material as possible is needed to get the right chemical composition of stainless steel [4]. Melting of scrap and ferro-alloys in the EAF (electric arc furnace) shown in Fig. 1 is the first step in the production of stainless steel. Scrap and ferro-alloys are charged into the furnace using large baskets. The lid is closed and the electrodes are lowered when powerful electric arcs start to melt the charge material mix. During the melting process, the arcs reach temperatures up to 3500 °C, and the molten steel can reach up to 1800 °C [5]. The power needed for this process varies between 50 and 80 MW depending on the EAF capacity. Additional injection of chemical energy in the form of carbon, oxygen or natural gas speeds up the melting process. After

Abbreviations: EAF, electric arc furnace; AOD, argon oxygen decarburization; VOD, vacuum oxygen decarburization; LF, ladle furnaces; MLP, multilayer perceptron; ANN, artificial neural network; BFGS, Broyden–Fletcher–Goldfarb–Shanno algorithm; SSE, sum of squares for error; MSE, mean squared error; RMSE, root mean squared error; MAE, mean absolute error; R^2, coefficient of determination.

* Corresponding author. School of Electrical Engineering, University of Belgrade, Bulevar kralja Aleksandra 73, 11000 Belgrade, Serbia. Tel.: +381 32 770 100; fax: +381 32 711 344.
E-mail address: dragoljubgajic@gmail.com (D. Gajic).

http://dx.doi.org/10.1016/j.energy.2015.07.068
0360-5442/

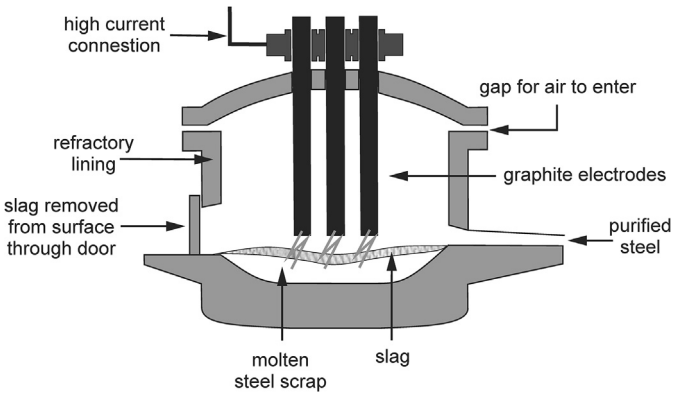

Fig. 1. Schematic representation of an electric arc furnace.

samples have been taken to check the chemical composition of the molten steel, the EAF is tilted to allow the slag, which is floating on the surface of the molten steel, to be poured off. The EAF is then tilted in the other direction and the molten steel poured (tapped) into a ladle. Final chemical composition of stainless steel is adjusted in the subsequent production stages by the AOD (argon oxygen decarburization), the VOD (vacuum oxygen decarburization) and the LF (ladle furnaces) to meet the standard quality requirements. The melting process in the EAF as the most energy-intensive step in the production of stainless steel has been investigated in a number of studies using various approaches with the goal to better understand the effect of various process parameters and thus further decrease the specific electrical energy consumption. For example, an optimal operating strategy can be determined taking into account different melting stages and electrodes position [6]. Understanding the influence of both gas burners [7] and direct reduced iron [8] on energy efficiency is also very important. Preheating of the charge material mix before its loading using off-gasses is among the most promising solutions for further reduction of energy consumption in the EAF [9].

The decision about the charge material mix composition is solely based on chemical composition, availability and price of different scrap materials. This study shows how the chemical composition of the charge material mix affects the specific electrical energy consumption and how electrical energy costs, as the second largest part of EAF operating cost, could be further lowered by taking into account such an impact as well when choosing an optimal charge material mix.

Nowadays, application of evolutionary algorithms such as ANNs (artificial neural networks) is broadly used to define a mathematical relationship between process inputs and outputs [10,11] as well as an efficient use of available resources [12]. This approach is based on the passing the inputs through the ANN and their transformation into the outputs using adequate activation function. The ANN consists of neurons that are classified in the input, hidden and output layers (Fig. 2). The hidden layer may have more than one layer.

The neurons are connected with neighboring neurons using the varying coefficients of connectivity, i.e. weights, which are optimally adjusted during training of ANN. The role of an artificial neuron is to activate the weighted sum of inputs from preceding layer of neurons including the bias neuron as given by the following equation:

$$y = f\left[\sum_{i=1}^{n} x_i w_i + b\right] \quad (1)$$

where b is the bias, x_i the input and w_i the weight from the ith neuron in the preceding layer and f the activation function. If necessary, the bias neuron may allow a shift of the activation function. The activation function typically falls into one of three categories: linear (or ramp), threshold and sigmoid.

In order to train a neural network, it is necessary to choose adequate activation function and adjust all the weights in such a way that the error between the desired output and the actual output is minimized. The training process also requires computation of the error derivative of the weights, i.e. how the error changes as each weight is increased or decreased slightly. The backpropagation algorithm is the most widely used method for determining the weights which are optimized moving from layer to layer in a direction opposite to the way activities propagate through the network. It uses the first-order techniques such as the gradient-descent method to optimize the weights in an iterative procedure. Quasi-Newton methods which use the second-order derivatives to find the optimal solution converge much faster. The second order derivatives are computed in a Hessian matrix, H, while the weight update is a product of the inverse Hessian matrix and the direction of the steepest descent. However, the computation of a Hessian matrix with all the second-order partial derivatives is time consuming. Therefore, approximations to the Hessian matrix are used to increase speed. In this work the BFGS (Broyden-Fletcher-Goldfarb-Shanno) algorithm [13] as the most efficient way of computing weight updates is used.

ANNs have been already proven as a suitable approach to various challenges related to the EAF operation such as temperature prediction [14,15] as well as simulation of its power load [16,17]. Olabi et al. [18] employed the backpropagation ANN and the Taguchi approach to design and to find out the optimum levels of the welding speed, the laser power and the focal position for CO_2 keyhole laser welding of medium carbon steel butt weld. Actually, the aim of the backpropagation algorithm is to reduce difference between actual and expected results, until the ANN learns the training data. The backpropagation algorithm send the signals forward, and then the errors are propagated backwards. Unlike the previous studies, the aim of this study was to use the feedforward ANNs, i.e. the MLP (multilayer perceptron), for modelling the relation between the specific electrical energy consumption and the chemical composition of the molten steel.

2. Experimental

2.1. Melts

Experimental melts used to build, test and validate our MLP model were run in the EAF at a melt shop in Italy, which is one of the global leaders in the manufacturing of stainless steel products. Its melt shop is based on modern technologies including the EAF, the AOD and VOD converters, the ladle furnaces and the continuous casters. In total 46 experimental melts were run with various chemical composition of the charge material mix during a couple of days in the summer 2014. Other important properties such as scrap type and density, injection of chemical energy as well as final temperature of the molten steel were kept as much as possible at a constant level during the melts in order to minimize their effect on the specific electrical energy consumption. The chemical composition of the molten steel was determined using the standard procedures in the melt shop laboratory.

2.2. Multilayer perceptron model

The feedforward ANNs were trained in order to construct the optimal network for estimation of the effect of the chemical components in the molten steel on the specific electrical energy consumption in the EAF. The content of carbon, chromium, nickel,

Please cite this article in press as: Gajic D, et al., Modelling of electrical energy consumption in an electric arc furnace using artificial neural networks, Energy (2015), http://dx.doi.org/10.1016/j.energy.2015.07.068

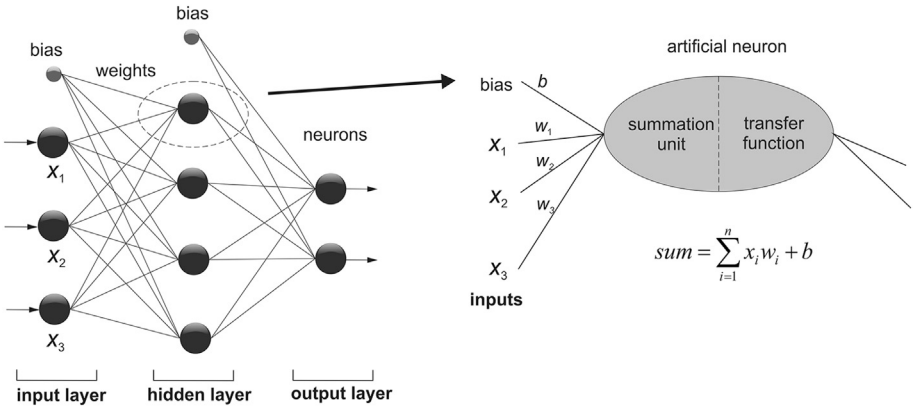

Fig. 2. The schematic representation of ANN and artificial neuron.

silicon and iron were defined as the inputs and varied in the range of 0.8–1.65%, 14.83–20.50%, 5.83–9.89%, 0.03–0.68% and 69.09–76.34%, respectively. The observed ranges of the inputs were in accordance with the declared values given in Table 1. The specific electrical energy consumption was chosen as the output and scaled to the range between 0 and 1000 kWh/t in order to maintain confidentiality of data.

MLP model with three layers was used for modelling the experimental data by applying BFGS algorithm. Both the weights and the activation functions are adjustable and they change during learning process in order to improve the predictive ability of the proposed network. In this study, the tested activation functions were hyperbolic tangent, linear and logistic sigmoid functions in the hidden and output layers. The outputs of the hidden layer are in fact the inputs of the output layer. The total number of performed experiments was 46 including the set data for training, testing and validation. The 32 experimental runs, i.e. about 70% of the total performed experiments represents the set of training data. For testing and validation of the neural network 15% of the total experiments each was used.

Statistica 8.0 (Stat Soft, Inc., Tulsa, USA) software was used for learning the ANN, i.e. for modelling the observed process. Learning process was performed until it reaches minimum value for SSE (sum of squares for error). The goodness of fit of the model was evaluated based on the values of MSE (mean squared error), RMSE (root mean squared error), MAE (mean absolute error), and coefficient of determination (R^2). The values of error parameters and coefficient of determination were calculated as follows (Eqs. (2)–(5)):

$$MSE = \frac{\sum_{i=1}^{n}\left(y_i^e - y_i^p\right)^2}{n} \tag{2}$$

$$RMSE = \sqrt{\frac{\sum_{i=1}^{n}\left(y_i^e - y_i^p\right)^2}{n}} \tag{3}$$

Table 1
Analyzed and declared values of stainless steel chemical composition.

Carbon	Chromium	Nickel	Silicon	Iron
Observed ranges				
0.8–1.65%	14.83–20.50%	5.83–9.89%	0.03–0.68%	69.09–76.34%
Declared ranges				
0–2%	13–22%	5–10%	0–1%	65–80%

$$MAE = \frac{\left|y_i^e - y_i^p\right|}{n} \tag{4}$$

$$R^2 = 1 - \left(\frac{\sum_{i=1}^{n}\left(y_i^e - y_i^p\right)^2}{\sum_{i=1}^{n}\left(y_i^e - \overline{y}_i^e\right)^2}\right) \tag{5}$$

where y_i^p is the predicted value, y_i^e is the experimental value, $\overline{y}_i^e$ is the average experimental value and n is the number of experiments.

Table 2
Training set of data.

Exp.	C, %	Cr, %	Ni, %	Si, %	Fe, %	E, kWh/t	
						Observed	Predicted
1	1.12	17.46	7.97	0.28	73.17	483	442
2	1.15	19.56	8.58	0.24	70.47	484	481
3	1.02	17.32	8.49	0.35	72.82	432	432
4	1.02	17.10	7.24	0.12	74.53	452	452
5	1.55	19.75	8.76	0.20	69.75	455	456
6	1.26	19.62	8.85	0.15	70.14	503	499
7	1.21	18.31	8.26	0.30	71.94	419	475
8	1.18	15.80	9.45	0.25	73.33	443	444
9	1.43	18.93	8.14	0.09	71.42	521	518
10	1.21	16.75	7.71	0.18	74.15	567	568
11	1.24	17.54	7.06	0.13	74.04	527	525
12	1.44	16.77	7.65	0.54	73.60	436	447
13	1.24	15.15	9.89	0.47	73.26	529	527
14	0.80	15.30	8.11	0.32	75.47	462	467
15	1.32	18.25	9.21	0.31	70.91	601	599
16	1.34	19.07	8.74	0.25	70.60	592	604
17	1.46	19.80	7.71	0.18	70.87	572	547
18	1.35	18.39	8.17	0.35	71.75	570	543
19	1.33	18.65	5.83	0.22	73.97	585	584
20	1.65	18.41	7.42	0.24	72.29	557	547
21	1.30	18.23	7.68	0.22	72.58	510	522
22	1.54	18.82	9.22	0.19	70.24	504	502
23	0.84	16.57	7.49	0.05	75.06	483	480
24	1.47	20.12	7.80	0.14	70.48	533	536
25	0.93	16.11	8.11	0.06	74.80	447	456
26	1.12	18.52	8.54	0.12	71.70	547	534
27	1.05	16.59	7.72	0.47	74.18	445	434
28	1.31	17.57	8.60	0.68	71.85	458	462
29	0.93	15.59	7.77	0.06	75.65	482	480
30	1.29	19.73	7.45	0.03	71.51	524	545
31	1.26	20.23	9.38	0.05	69.09	477	481
32	1.33	20.50	8.11	0.03	70.03	509	522

Please cite this article in press as: Gajic D, et al., Modelling of electrical energy consumption in an electric arc furnace using artificial neural networks, Energy (2015), http://dx.doi.org/10.1016/j.energy.2015.07.068

Table 3
Testing set of data.

Exp.	C, %	Cr, %	Ni, %	Si, %	Fe, %	E, kWh/t	
						Observed	Predicted
33	1.17	19.55	7.49	0.04	71.76	548	552
34	1.42	19.04	7.38	0.09	72.08	542	546
35	1.42	17.13	7.21	0.37	73.88	426	439
36	1.35	18.28	8.25	0.20	71.93	543	548
37	1.47	18.84	7.97	0.32	71.41	567	580
38	1.27	18.88	7.61	0.15	72.10	571	557
39	1.38	17.87	7.67	0.22	72.87	564	585

Table 4
Validation set of data.

Exp.	C, %	Cr, %	Ni, %	Si, %	Fe, %	E, kWh/t	
						Observed	Predicted
40	1.12	14.83	7.38	0.35	76.34	473	443
41	1.20	16.87	7.69	0.16	74.08	564	570
42	1.62	19.45	7.04	0.32	71.57	675	645
43	1.07	16.70	7.57	0.12	74.55	521	524
44	1.40	18.79	8.04	0.16	71.61	482	508
45	1.36	19.78	7.89	0.07	70.91	534	526
46	1.38	19.30	8.32	0.20	70.81	475	478

3. Results and discussion

Melting of the charge material mix (scrap and ferro-alloys) in the EAF is a very energy-intensive process [19]. In the production of stainless steel, apart from iron, carbon and silicon, the presence of chromium and nickel in the charge material mix is also evident. The chemical composition of the molten steel of course depends on the composition of the charge material mix. The content of all metals in the molten steel should be in the allowed range in order to be able to produce a specific stainless steel grade in the subsequent production stages. The consumed electrical energy depends on the alloying element contents in the charge material mix as well as its density, layering and injection of chemical energy. Due to these reasons, the aim of this study was to investigate effect of the contents of carbon, chromium, nickel, silicon and iron on the specific electrical energy consumption. Density and layering of scrap in the charge material mix as well as injection of chemical energy during the melting process were pretty well kept at a constant level during the experimental melts.

Table 5
Evaluation of the goodness of fit statistics.

	Training	Test	Validation	Total
R^2	0.91	0.95	0.92	0.92
MAE	9.48	11.61	15.10	10.54
MSE	241.87	153.93	369.31	247.88
RMSE	15.55	12.41	19.22	15.74

The observed and predicted values of the response expressed in kWh/t for training data of MLP model are given in Table 2. Total sum of each combination of the independent variables is equal to 100%. The experimental values of the specific electrical energy consumption varied in the range of 419–601 kWh/t.

Two additional sets of data used for testing and validation of MLP network are given in Table 3 and Table 4, respectively. The obtained experimental data and MLP predicted values of the specific electrical energy consumption are also presented in these tables. Based on these data the prediction ability of the proposed model was evaluated by classification of the data from the same class as the training data.

From Table 4, it can be seen that the specific electrical energy consumption was in the range of 426–571 kWh/t for testing set of data, i.e. 472–675 kWh/t for validation set of data. The optimal MLP 5-5-1 network obtained after 89 cycles is presented in Fig. 3a. Such an architecture indicates that the MLP model has the 5 inputs, 5 neurons in the hidden layer and 1 output. In each training cycle the entire training set was passed through the network and its error calculated. In Fig. 3a, it can be seen that there is also a bias in both input and hidden layers. The development of SSE in training and testing processes is also presented in Fig. 3b. The chosen activation functions in the hidden and output layers are hyperbolic tangent and linear function, respectively.

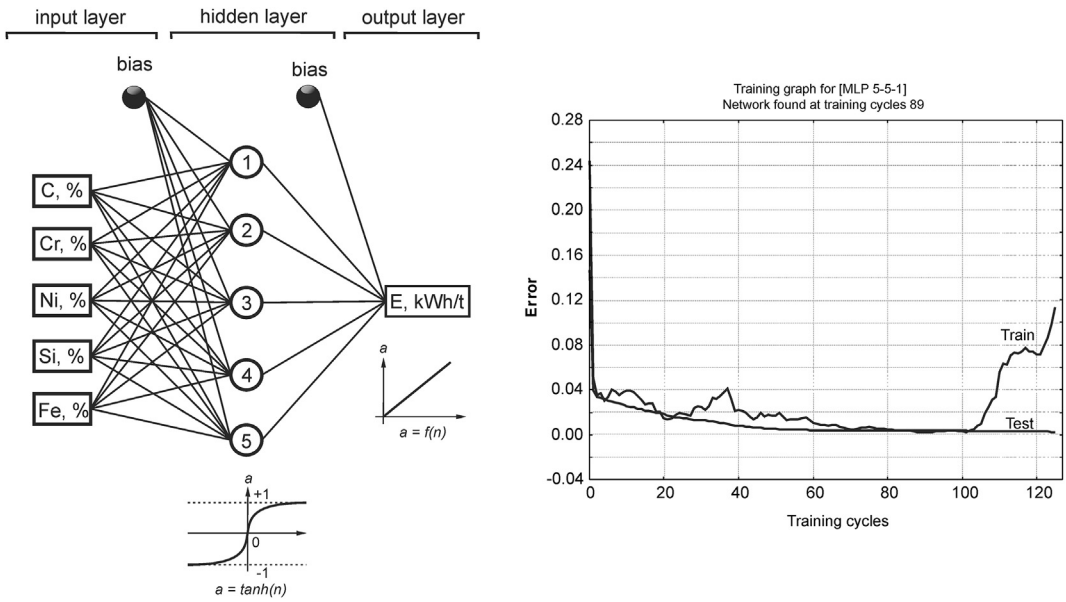

Fig. 3. Architecture of the optimal neural network with diagram of development of SSE in training and testing process.

Please cite this article in press as: Gajic D, et al., Modelling of electrical energy consumption in an electric arc furnace using artificial neural networks, Energy (2015), http://dx.doi.org/10.1016/j.energy.2015.07.068

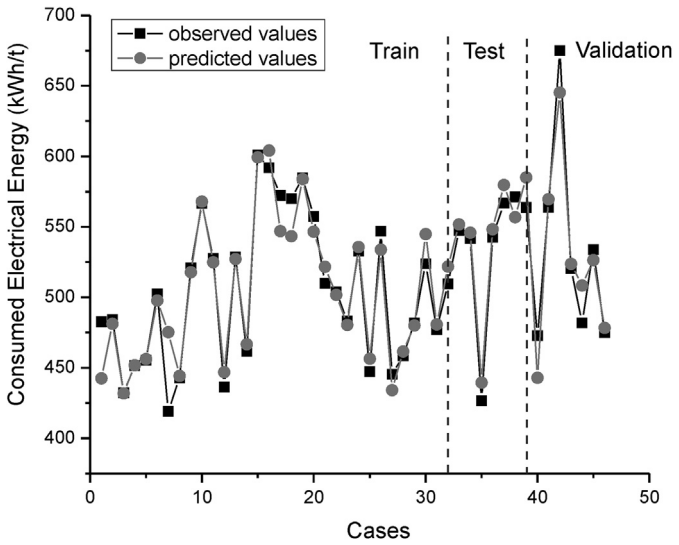

Fig. 4. Comparison of MLP predicted values with measured data.

The goodness of fit of the proposed model was evaluated based on the values of errors and coefficients of determination (Table 5) [20]. The value $R^2 = 0.91$ for training of the neural network indicates that 91% of variation in the specific electrical energy consumption could be explained using the proposed model. For testing and validation of the neural network, the calculated values of R^2 are higher than 0.9 that indicates adequacy of the model proposed for prediction of the specific electrical energy consumption in the EAF. The highest value was achieved during testing of the MLP model. An overall R^2 value of 0.92 is quite acceptable for the proposed model.

The prediction ability of MLP model for training, testing and validation is presented in Fig. 4. Fig. 4 indicates the consistent and commendable concurrency of the predicted values with the actual values for the entire range of operation. Actually, the sensitivity and robustness of the model to predict the values of the specific electrical energy consumption with an excellent accuracy was achieved.

The interaction effects between carbon content and all remaining element contents are presented in Fig. 5. In Fig. 5a, two local maximums can be noticed for the interaction between carbon and chromium. An increase in the specific electrical energy consumption was noticed when carbon content is higher than 1.2% and chromium content low in the molten steel. This is in accordance with the fact that the melting point of carbon of 3500 °C [21] is significantly higher than the melting point of chromium of 1830 °C [22]. Similar observations can be noticed when chromium content is higher than 19%. In Fig. 5b, the effect of carbon and nickel content is given in the form of contour diagram. In this case, nickel content does not have significant effect on the electrical energy consumption, because its melting point is among the lowest values (1455 °C) of all other investigated elements [23]. The maximum of the response surface is noticed for carbon content higher than 1.6% and low nickel content. The functional dependency between carbon and silicon contents given in Fig. 5c shows a similar trend of increased electrical energy consumption when silicon content is in the middle zone (0.4%). Due to lower melting point of silicon (1420 °C) [24], the main contribution in the increase of the specific electrical energy consumption has carbon content. The contour diagram in Fig. 5d represents the interaction effect between carbon and iron contents. The significant changes in the electrical energy consumption is not clearly expressed as in the previous cases, but it

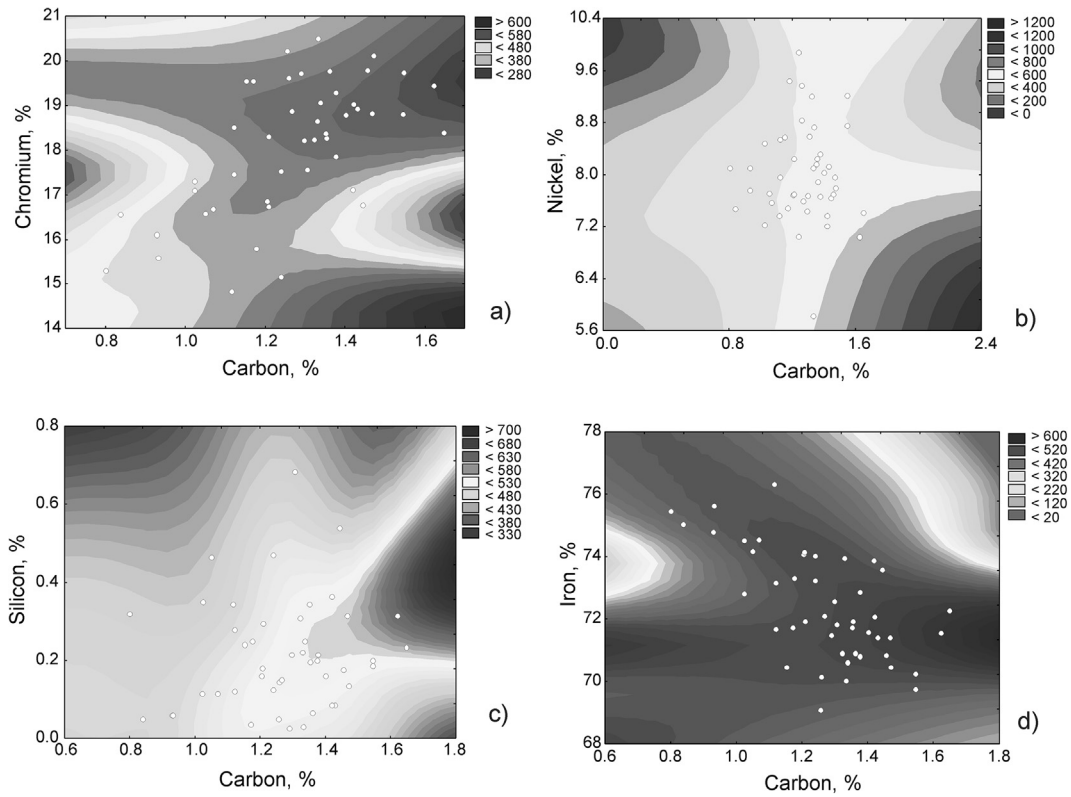

Fig. 5. The interaction effects between carbon content and other element contents on the specific electrical energy consumption.

Please cite this article in press as: Gajic D, et al., Modelling of electrical energy consumption in an electric arc furnace using artificial neural networks, Energy (2015), http://dx.doi.org/10.1016/j.energy.2015.07.068

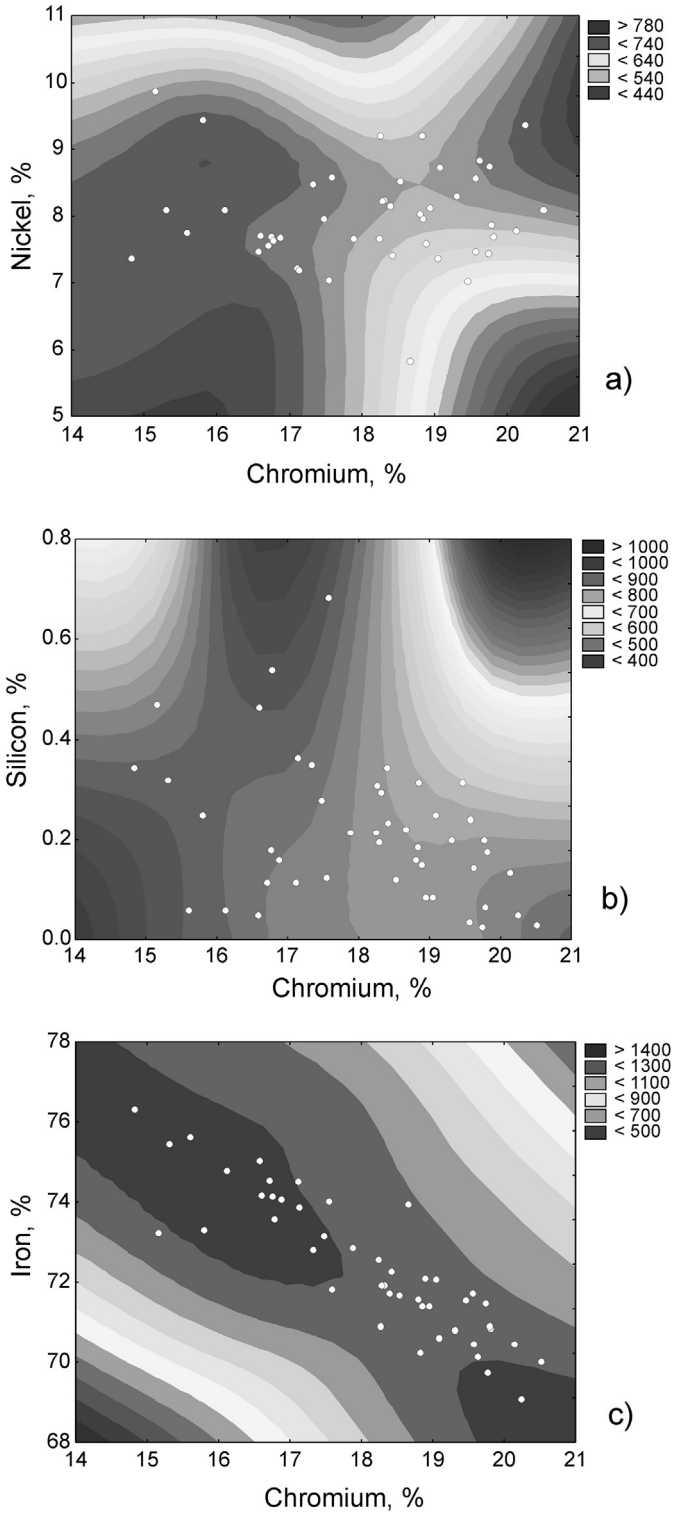

Fig. 6. The interaction effects between chromium content and other element contents on the specific electrical energy consumption.

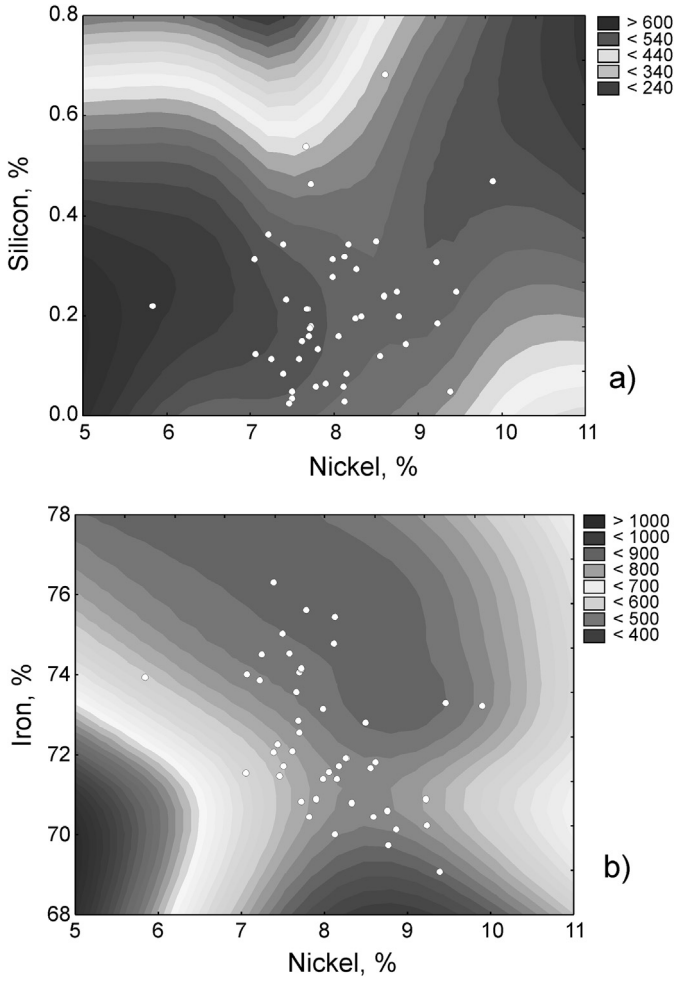

Fig. 7. The interaction effects between nickel content and other element contents on the specific electrical energy consumption.

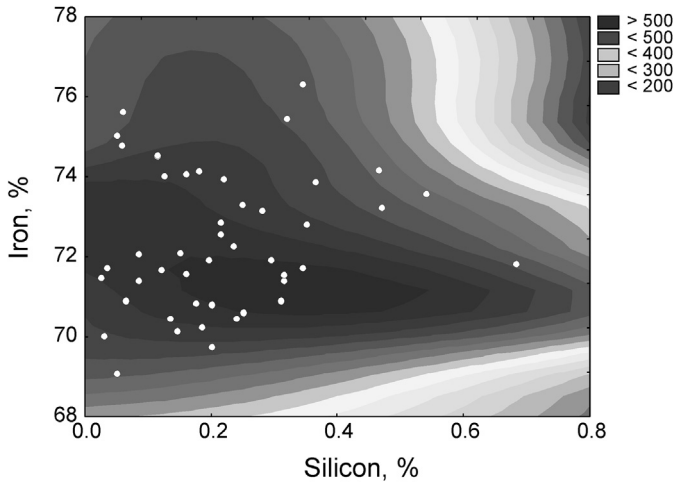

Fig. 8. The interaction effects between silicon and iron content on the specific electrical energy consumption.

is higher when iron content is around 71% and carbon content high. Based on the literature data it can be seen that melting point of pure iron (1535 °C) is lower than the one of carbon [25]. Thus, carbon content has a greater impact on the specific electrical energy consumption than iron content in the charge material mix.

The interaction effects between chromium content and other element contents is given in Fig. 6. The interaction between chromium and nickel contents has a local maximum when chromium content is high and nickel content low (Fig. 6a). Outside this area,

Please cite this article in press as: Gajic D, et al., Modelling of electrical energy consumption in an electric arc furnace using artificial neural networks, Energy (2015), http://dx.doi.org/10.1016/j.energy.2015.07.068

the minimum electrical energy is necessary to melt the charge material mix in the EAF. In Fig. 6b, the significant effect of chromium was confirmed when silicon content is higher than 0.6%, while the change in the specific electrical energy consumption is negligible when silicon content is low. The interaction between chromium and iron contents is presented in Fig. 6c. The local maximum was not noticed in this contour diagram. For this functional dependency, the shape of response surface looks like a ridge.

The interaction effects between nickel content and other element contents are presented in Fig. 7. By increasing nickel content in the molten steel, the specific electrical energy consumption is decreased when silicon content is low (Fig. 7a). From this figure, it can be seen that the significant effect of nickel content was achieved when silicon content is high. In Fig. 7b, the interaction between nickel and iron contents has a local maximum when both these contents are low, i.e. the specific electrical energy consumption was decreased with an increase in nickel content and when iron content is low.

In Fig. 8, the interaction effects between silicon and iron contents on the specific electrical energy consumption is presented. The maximum was achieved when silicon and iron contents were in the range of 0.2–0.5% and 70–72%, respectively. By comparison of the both melting points, more electrical energy is necessary for melting pure iron. This fact also can be noticed based on the shape of response surface. For small changes in iron content, the electrical energy consumption significantly increases.

Based on the analysis of the contour diagrams, it can be concluded that carbon content has the greatest impact on the specific electrical energy consumption in comparison with other alloying elements. But also, the effect of other elements in the charge material mix cannot be omitted. The decreasing order of the impact on the specific electrical energy consumption can be presented in the following way: carbon content > chromium content > iron content > nickel content > silicon content.

In this paper an MLP model has been applied to predict the electrical energy consumption based on the chemical composition of the charge material mix. To estimate the effect of the most important process parameters of EAF on the electrical energy consumption some other models have also been developed. A statistical model [26] based on average values from many EAFs and used for performance comparison of different furnaces takes into account the effect of different scrap materials only roughly. The model was tested on individual heats for prediction of electrical energy consumption and showed low prediction accuracy. The model coefficients were also compared to thermodynamical calculations [27], and shown to be quite similar. One of the first company to use multivariate statistics in steel industry is Dofasco in Canada [28,29]. Also some other models for scrap optimization have been developed and published [30,31]. These models are in the form of spreadsheets and based on price, yield and density of different scrap materials. Of course, the performances of all these models including the one described in this paper depend on the accuracy of assumed scrap properties which are usually estimated with traditional statistical methods.

4. Conclusion

Melting of the charge material mix in the EAF is one of the most energy-intensive industrial processes. The effect of the chemical composition of the molten steel and thus the charge material mix on the specific electrical energy consumption was modelled using a novel ANN approach. The optimal neural network MLP 5-5-1 with hyperbolic tangent in the hidden layer and linear function in the output layer was obtained after 89 cycles. The proposed model has the ability to successfully predict the values of the electrical energy consumption in function of the chemical composition of the charge material mix. The MLP predicted values of the specific electrical energy consumption were in agreement with the experimentally obtained data. The highest impact on the electrical energy consumption has carbon content present in the charge material mix. The proposed model confirmed that the chemical composition of the charge material mix plays an important role when it comes to electrical energy consumption in the EAF. Based on the obtained results the model can be used to support decisions when making optimal recipes for the charge material mix in order to lower electrical energy costs as one of the biggest operating costs in the EAF.

Acknowledgments

This study was supported by the FP7 Marie Curie ITN “EnergySmartOps”, Contract No: PITN-GA-2010-264940, the FP7 Marie Curie ITN “InnHF”, Contract No: PITN-GA-2011-289837 and the Erasmus Mundus Action II EUROWEB+, Contract No: 552125-EM-1-2014-1-SE-ERA MUNDUS-EMA21.

References

[1] Bisio G, Rubatto G, Martini R. Heat transfer, energy saving and pollution control in UHP electric-arc furnaces. Energy 2000;25(11):1047–66.
[2] Luiten EE, Blok K. Stimulating R&D of industrial energy-efficient technology; the effect of government intervention on the development of strip casting technology. Energy Policy 2003;31(13):1339–56.
[3] Mortensen LF, Mountford H, Braathen NA, Cheong HS, Christensen N, Geyer-Allely E, et al. OECD environmental outlook. Paris: OECD Publishing; 2001. p. 221.
[4] Outokumpu. Handbook of stainless steel. Espoo Outokumpu Oyj; 2013.
[5] Hadera H, Harjunkoski I, Sand G, Grossmann IE, Engell S. Optimization of steel production scheduling with complex time-sensitive electricity cost. Comput Chem Eng 2015;76:117–36.
[6] Hocine L, Yacine D, Kamel B, Samira KM. Improvement of electrical arc furnace operation with an appropriate model. Energy 2009;34(9):1207–14.
[7] Kirschen M, Risonarta V, Pfeifer H. Energy efficiency and the influence of gas burners to the energy related carbon dioxide emissions of electric arc furnaces in steel industry. Energy 2009;34(9):1065–72.
[8] Kirschen M, Badr K, Pfeifer H. Influence of direct reduced iron on the energy balance of the electric arc furnace in steel industry. Energy 2011;36(10):6146–55.
[9] Lee B, Sohn I. Review of innovative energy savings technology for the electric arc furnace. JOM 2014;66(9):1581–94.
[10] Benyounis KY, Olabi AG. Optimization of different welding processes using statistical and numerical approaches–a reference guide. Adv Eng Softw 2008;39(6):483–96.
[11] Savic IM, Stojiljkovic ST, Stojanovic SB, Moder K. Modeling and optimization of Fe (III) adsorption from water using bentonite clay: comparison of central composite design and artificial neural network. Chem Eng Technol 2012;35(11):2007–14.
[12] Savic IM, Nikolic VD, Savic-Gajic IM, Nikolic LB, Ibric SR, Gajic DG. Optimization of technological procedure for amygdalin isolation from plum seeds (*Pruni domesticae semen*). Front Plant Sci 2015;6:276.
[13] Shanno DF. Conditioning of Quasi-Newton methods for function minimization. Math Computation 1970;24:647–57.
[14] Kordos M, Blachnik M, Wieczorek T. Temperature prediction in electric arc furnace with neural network tree. In: Artificial neural networks and machine learning–ICANN. Berlin: Springer Berlin Heidelberg; 2011. p. 71–8.
[15] Fernández JMM, Cabal VA, Montequin VR, Balsera JV. Online estimation of electric arc furnace tap temperature by using fuzzy neural networks. Eng Appl Artif Intel 2008;21(7):1001–12.
[16] Wang F, Jin Z, Zhu Z. Modeling and prediction of electric arc furnace based on neural network and chaos theory. In: Advances in neural networks–ISNN. Berlin: Springer Berlin Heidelberg; 2005. p. 819–26.
[17] Chang GW, Chen CI, Liu YJ. A neural-network-based method of modeling electric arc furnace load for power engineering study. IEEE Trans Power Syst 2010;25(1):138–46.
[18] Olabi AG, Casalino G, Benyounis KY, Hashmi MSJ. An ANN and Taguchi algorithms integrated approach to the optimization of CO_2 laser welding. Adv Eng Softw 2006;37(10):643–8.
[19] Price L, Sinton J, Worrell E, Phylipsen D, Xiulian H, Ji L. Energy use and carbon dioxide emissions from steel production in China. Energy 2002;27(5):429–46.
[20] Sinha K, Chowdhury S, Saha PD, Datta S. Modeling of microwave-assisted extraction of natural dye from seeds of *Bixa orellana* (Annatto) using response surface methodology (RSM) and artificial neural network (ANN). Ind Crop Prod 2013;41:165–71.
[21] Saevarsdottir G, Tao PC, Stefansson H, Harvey W. Potential use of geothermal energy sources for the production of lithium-ion batteries. Renew Energy 2014;61:17–22.

Please cite this article in press as: Gajic D, et al., Modelling of electrical energy consumption in an electric arc furnace using artificial neural networks, Energy (2015), http://dx.doi.org/10.1016/j.energy.2015.07.068

[22] Zhang G, Li J, Chen Y, Xiang H, Ma B, Xu Z, et al. Encapsulation of copper-based phase change materials for high temperature thermal energy storage. Sol Energy Mat Sol C 2014;128:131–7.
[23] Meshkani F, Rezaei M. A highly active and stable chromium free iron based catalyst for H_2 purification in high temperature water gas shift reaction. Int J Hydrogen Energy 2014;39(32):18302–11.
[24] Zhou X, Liu Y, Li X, Gao Q, Liu X, Fang Y. Topological morphology conversion towards SnO_2/SiC hollow sphere nanochains with efficient photocatalytic hydrogen evolution. Chem Commun 2014;50(9):1070–3.
[25] Sorgenfrei M, Tsatsaronis G. Design and evaluation of an IGCC power plant using iron-based syngas chemical-looping (SCL) combustion. Appl Energy 2014;113:1958–64.
[26] Köhle S. Recent improvements in modelling energy consumption of electric arc furnaces. In: Proceedings of 7th European electric steelmaking conference. Venice, Italy, 26–29 May, vol. 1; 2002. p. 305–14.
[27] Pfeifer H, Kirschen M. Thermodynamic analysis of EAF energy efficiency and comparison with a statistical model of electric energy demand. In: Proceedings of 7th European electric steelmaking conference. Venice, Italy, 26–29 May, vol. 1; 2002. p. 413–28.
[28] Vaculik V, Maccuish RB, Dudzic MS, Miletic I, Hough MJ, Smith KB. Innovative monitoring technology improves caster operation at Dofasco. Iron Steelmaker 2001;28(9):23–8.
[29] Quinn V. Improving the desulphurization process using adaptive multivariate statistical modelling. AISE Steel Technol 2002;79(10):37–41.
[30] Bokan R, Jones J, Kemeny F. Improved understanding of feed materials with respect to optimizing EAF operations. In: Proceedings of 60th electric furnace conference. San Antonio, Texas, USA, 10–13 November; 2002. p. 47–57.
[31] Martin B, Whipp R. Scrap optimization strategy for a new era of steelmaking. Iron Steelmaker 2000;30(6):43–8.

Please cite this article in press as: Gajic D, et al., Modelling of electrical energy consumption in an electric arc furnace using artificial neural networks, Energy (2015), http://dx.doi.org/10.1016/j.energy.2015.07.068